

Pressure-Stabilized Low-Spin State for Binuclear Iron(III) Spin-Crossover Compounds

Shinya Hayami,* Yuko Hosokoshi,† Katsuya Inoue,† Yasuaki Einaga,†† Osamu Sato,†† and Yonezo Maeda*

Department of Chemistry, Faculty of Sciences, Kyushu University, 6-10-1 Hakozaki, Higashi-ku, Fukuoka 812-8581

†Institute for Molecular Science, Myodaiji, Okazaki 444-8585

††Kanagawa Academy of Science and Technology, KSP Bldg. East 412, 3-2-1 Sakado, Takatsu-ku, Kawasaki, Kanagawa 213-0012

(Received July 4, 2001)

Binuclear iron(III) spin-crossover complexes with salten ligand $[Fe_2(salten)_2(L)](BPh_4)_2$ were synthesized and characterized by single-crystal X-ray diffraction, Mössbauer spectra, magnetic susceptibilities and electronic spectra, where H_2salten is a pentadentate ligand derived from salicylaldehyde and 3,3′-diaminodipropylamine and L is a didentate axial ligand (az = azobis(4-pyridine) and cc = 4,4′-vinylenebis(pyridine)). The structures of $[Fe_2(salten)_2(az)](BPh_4)_2$ (**1**) and $[Fe_2(salten)_2(cc)](BPh_4)_2$ (**2**) were determined at both 100 K and 298 K. Crystal data for **1** at 100 K: $C_{98}H_{94}O_4N_{10}B_2Fe_2$, monoclinic, space group $P2_1/c$, $Z = 2$, $a = 15.986(2)$ Å, $b = 15.825(2)$ Å, $c = 16.441(2)$ Å, $\beta = 107.902(2)°$, $V = 3957.8(8)$ Å^3. Crystal data for **2** at 100 K: $C_{100}H_{96}O_4N_8B_2Fe_2$, monoclinic, space group $P2_1/a$, $Z = 2$, $a = 16.4296(8)$ Å, $b = 15.747(1)$ Å, $c = 16.637(1)$ Å, $\beta = 109.2375(9)°$ and $Z = 2$. The complexes **1** and **2** exhibited the spin-crossover behavior depending on temperature within the temperature range of 200 to 350 K, and rapid spin equilibrium behavior was observed by means of Mössbauer spectroscopy at 293 K. The complexes **1** and **2** also exhibited a pressure-induced spin transition between the rapid spin equilibrium state and low-spin state at 300 K. Such a pressure-induced spin transition has not been reported earlier.

The first transition metal complexes with d^4, d^5, d^6 and d^7 electron configuration are usually classified into two categories according to the strength of ligand field against the mean spin-pairing energy, i.e., high-spin (HS) and low-spin (LS) complexes. In some cases, however, if the ligand field strength is comparable to the mean spin-pairing energy, the complexes exhibit a spin transition with the change in temperature[1,2] or pressure.[3] In particular, a number of spin-crossover iron(II) and iron(III) complexes have been studied, the spin-crossover iron(II) complexes have been also exhibited a spin transition from low-spin to metastable high-spin states by light irradiation at low temperature. This light-induced spin-transition effect is termed LIESST (light-induced excited spin-state trapping); the high-spin species remain trapped by light irradiation.[4] The difference in metal-ligand bond length $\Delta r°_{HL}$ and the zero-point energy difference $\Delta E°_{HL}$ of spin-crossover iron(III) complexes are smaller than those of iron(II) complexes, so the lifetime of the light-induced high-spin state in the iron(III) spin-crossover complexes is very short even at low temperature.[5] Furthermore, ligand-driven light-induced spin changes (LD-LISC) in the spin-crossover iron(II) complexes have been reported by Zarembowitch et al.[6] The spin transition of LD-LISC is classified in a new strategy which consists in varying the ligand field strength under photochemical *cis–trans* isomerization of the ligand. The phenomenon has been observed by using 4-styrylpyridine derivatives at relatively high temperature. One of the advantages of this LD-LISC effect is that the spin transition is driven by photoisomerization, and the photoisomerization ligands may be applied to the compounds having functions such as dynamical electronic states (spin-crossover or mixed-valence etc.).[7] Furthermore, the spin-crossover iron(II) complexes are particularly well suited for pressure studies because the difference in volume, $\Delta V°_{HL} = V_{HS} - V_{LS}$, between HS and LS complexes is comparatively large due to the difference in metal-ligand bond lengths, $\Delta r°_{HL} = r_{HS} - r_{LS} \approx 0.16 - 0.21$ Å; the external pressure also affect the kinetics of the HS → LS relaxation.[8,9] The application of pressure can be a powerful tool to investigate the interplay between spin transition and structural phase transition because pressure usually stabilizes the LS state.

Recently, we have reported iron(III) complexes whose spin transition is driven by photoisomerization.[10] Hence, we report for the first time that the binuclear spin-crossover iron(III) complexes **1** with photoisomerization ligands az and **2** with cc[7a] (Scheme 1) exhibit spin transition induced by pressure.

Experimental

Syntheses. The ligand az = azobis(4-pyridine) was prepared by the following procedure described previously.[11] The ligand cc = 4,4′-vinylenebis(pyridine) was purchased from Aldlich-Co. and was used without any purification.

$[Fe_2(salten)_2(az)](BPh_4)_2$ (1). H_2salten was prepared by adding a solution of 3,3′-diaminodipropylamine (0.21 g, 2 mmol) in methanol (25 mL) to a solution of salicylaldehyde (0.49 g, 4

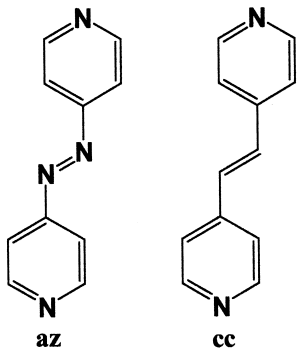

Scheme 1.

mmol) in methanol (25 mL) under stirring. The solution turned yellow immediately; this solution was stirred at room temperature for 2 h. Then a solution of $Fe(NO_3)_3 \cdot 9H_2O$ (0.81 g, 2 mmol) in methanol (10 mL) was added dropwise to the yellow solution, producing a dark purple solution. To the solution was added a solution of az (0.19 g, 1 mmol) in methanol (10 mL) and this mixture was stirred for 1 h. Then to the solution was added a solution of sodium tetraphenylborate (2.05 g, 6 mmol) in methanol (10 mL) and this mixture was stirred for 1 h. The solution was filtered and taken to dryness under reduced pressure at room temperature. The dark purple solid materials were recrystallized from an acetone–ethanol solution. The crystals were washed with ethanol and then with ether, and dried under vacuum at room temperature. Anal. Calcd for $C_{98}H_{94}O_4N_{10}B_2Fe_2$ (**1**): C, 73.14; H, 5.89; N, 8.71%. Found: C, 72.59; H, 5.87; N, 8.58%.[12]

$[Fe_2(salten)_2(cc)](BPh_4)_2$ (2). The preparative method for the complex **2** is similar to that described above. Anal. Calcd for $C_{100}H_{96}O_4N_8B_2Fe_2$ (**2**): C, 74.73; H, 6.02; N, 6.97%. Found: C, 75.14; H, 6.00; N, 6.72%.[12]

Physical Measurements. The magnetic susceptibilities of the polycrystalline samples were measured by a Quantum Design MPMS5S SQUID magnetometer at 0.5 T. Temperatures were controlled over the range 1.8–350 K. Both heating and cooling rates were controlled and magnetic data for one loop were constantly collected in about 10 h. Effective magnetic moments were calculated by use of the formula $\mu_{eff} = (8\chi_m T)^{1/2}$, where χ_m is molar susceptibility after applying a diamagnetic correction using Pascal's constants.

Mössbauer spectroscopy was effected by use of a constant-acceleration spectrometer (Austin Science Associates (ASA)). Data were stored in a 1024-channel pulse height analyzer, Type 5200 (Inotech, Inc.). The temperatures were monitored with a calibrated copper vs constantan thermocouple within a variable-temperature cryostat, Type ASAD-4V-(ASA). A cobalt-57 source of 10 mCi diffused into palladium foil was used for the absorption measurement. Some of the spectra were fitted to the Lorentzian line shape by using a least-squares method at the Computer Center, Kyushu University. Isomer shifts are reported with respect to the centroid of the spectrum of iron foil enriched with ^{57}Fe.

The pressure system used a small high-pressure clamp cell made of Cu-Ti alloy which can be equipped to a Quantum Design SQUID magnetometer.[13] The inner pressure of the clamp cell has been calibrated by the superconducting transition temperature of Pb. The maximum pressure maintained is ca. 8 kbar, the reproducibility is good, and the pressure deviation depending on temperature in the cell is within ca 0.3 kbar. As pressure-transmitting medium, a fluorine oil (Montefluos, H-VAC140/13) was used.

X-ray Crystallography. Brown platelet crystals of **1** and **2** having approximate of $0.2 \times 0.2 \times 0.05$ and $0.4 \times 0.4 \times 0.1$ mm, respectively, were mounted in a glass capillary. The temperatures of the crystals were slowly decreased from room temperature to 100 K, and then the X-ray structure analyses were carried out. All measurements were made on a Rigaku RAXIS-RAPID Imaging Plate diffractometer with graphite monochromated Mo-$K\alpha$ radiation. The data were collected at 100 K to a maximum 2θ value of 55.0°. For **1**, of the 32016 reflections which were collected, 25844 were unique ($R_{int} = 0.090$) and 8412 with $I > 3\sigma(I)$ were used to solve the structure with SIR92. Final R values gave $R1 = 0.065$ for $I > 3\sigma(I)$, $R = 0.089$ and $R_w = 0.144$ for all data; linear absorption coefficient $\mu(MoK\alpha) = 4.29\ cm^{-1}$. For **2**, of the 73402 reflections which were collected, 64388 were unique ($R_{int} = 0.139$) and 9001 with $I > 3\sigma(I)$ were used to solve the structure with SIR92. Final R values gave $R1 = 0.044$ for $I > 3\sigma(I)$, $R = 0.068$ and $R_w = 0.093$ for all data; linear absorption coefficient $\mu(MoK\alpha) = 4.17\ cm^{-1}$. The non-hydrogen atoms were refined anisotropically. Hydrogen atoms were included but not refined. Selected crystal data are given in Table 1.

Results and Discussion

Magnetic Susceptibilities. The temperature dependencies of magnetic susceptibilities of the single crystals were measured in the temperature range of 1.8 to 350 K and the effective magnetic moments per one iron for the complexes are shown in Fig. 1. The values of the magnetic moments for **1** and **2** are almost constant ($\mu_{eff} = 2.0\ \mu_B$) in the temperature range of 1.8–200 K, and are in the range of values expected for low-spin iron(III) ions. The values for **1** and **2** increase gradually from ca. 2.0 μ_B at 200 K to ca 4.4 μ_B and 3.9 μ_B at 350 K, respectively. The magnetic behavior for the increasing and decreasing temperature sequences is practically the same, indicating that the spin transition between high- and low-spin states is not associated with a thermal hysteresis. The results suggest that **1** and **2** can be classified as a continuous type of the spin transition. The value of the magnetic moment of **1** at 350 K (ca. 4.4 μ_B) is larger than that of **2** (ca. 3.9 μ_B), i.e. the ligand field strength of **2** with cc (vinyl group) is stronger than that of **1** with az (azo group). A value of ca. 2.0 μ_B is characteristic of an iron(III) complex in the low-spin state; a value of

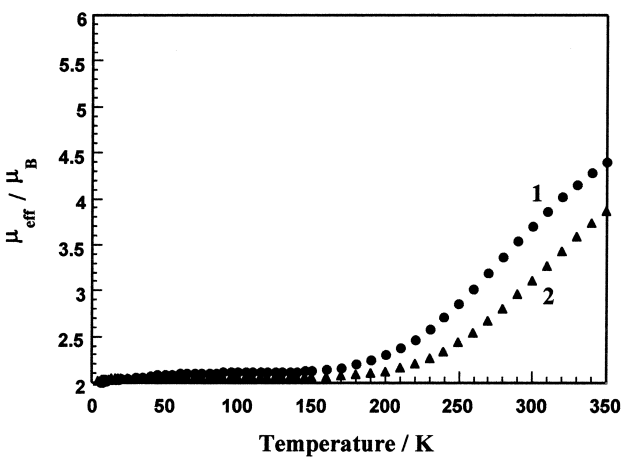

Fig. 1. Temperature dependence of the effective magnetic moments of **1** (●) and **2** (▲).

Table 1. Crystallographic Data for Complexes at 298 and 100 K

Complexes	**1**		**2**	
	T = 298 K	T = 100 K	T = 298 K	T = 100 K
Empirical formula	$C_{98}H_{94}O_4N_{10}B_2Fe_2$		$C_{100}H_{96}O_4N_8B_2Fe_2$	
Formula weight	1609.20		1607.22	
Crystal dimensions/mm	0.20 × 0.30 × 0.10		0.20 × 0.20 × 0.10	
Crystal system	monoclinic		monoclinic	
Space group	$P2_1/c$ (#14)		$P2_1/a$ (#14)	
a/Å	16.422(7)	15.986(2)	16.554(8)	16.4296(8)
b/Å	16.005(6)	15.825(2)	15.877(3)	15.747(1)
c/Å	16.565(8)	16.441(2)	16.823(3)	16.637(1)
β/°	108.47(3)	107.902(2)	109.20(2)	109.2375(9)
V/Å^3	4129(2)	3957.8(8)	4175(1)	4063.9(4)
Z	2	2	2	2
D_{calcd}/g cm^{-3}	1.294	1.350	1.278	1.313
$R1$		0.065[b)]		0.044[b)]
R	0.075[a)]	0.089[b)]	0.051[a)]	0.068[b)]
R_w	0.060[a)]	0.144[b)]	0.040[a)]	0.093[b)]

a) R and R_w values were gave for $I > 3\sigma(I)$. b) $R1$ values were gave for $I > 3\sigma(I)$, and R and R_w for all data.

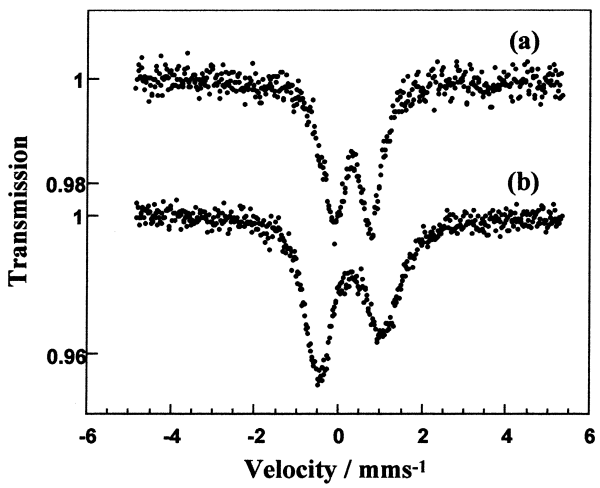

Fig. 2. Mössbauer spectra of **1** (a) at 293 K and (b) at 80 K.

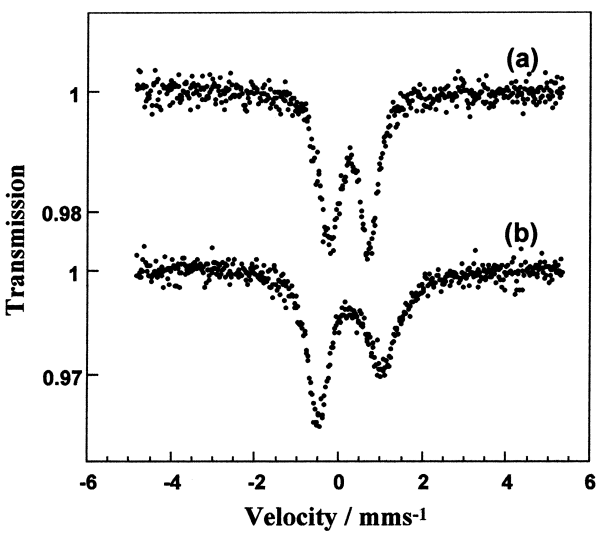

Fig. 3. Mössbauer spectra of **2** (a) at 293 K and (b) at 80 K.

5.9 μ_B would be expected for iron(III) complexes in the high-spin state. The values of the magnetic moments of **1** and **2** were smaller than typical values of high-spin (S = 5/2). The complexes **1** and **2** are in the low-spin state (S = 1/2) below 200 K. These observations suggest that the complexes are the mixtures of high- and low-spin species (S = 1/2 and S = 5/2) or that the complexes show rapid spin-equilibrium behavior (S = 1/2 ↔ S = 5/2).[2c,d]

Mössbauer Spectra. The variable temperature Mössbauer spectra of **1** and **2** are shown in Figs. 2 and 3, respectively. The Mössbauer parameters derived from the spectra are given in Table 2. Typical absorptions of low-spin iron(III) ions with the large quadrupole splitting ($Q.S.$ = 1.525 mms^{-1}) and small isomer shift ($I.S.$ = 0.251 mms^{-1}) were observed for the spectrum of **1** at 80 K, the spin state (low-spin) expected from the spectrum agreed with that expected from the magnetic measurements (2.0 μ_B). The value of the quadrupole splitting of **1** at 80 K is less than that of the iron(III) complexes with salten reported previously (2.72 mms^{-1});[2a] the difference seems to result from the change in q_{lat} (the electron field gradient due to lattice contribution) because the iron atoms have a distorted octahedral coordination. The spectrum at 80 K is very broad and antisymmetric, and the exact reason for the broadening is not clear; however, spin-lattice relaxation effects on $^2T_2$ may be induced because of the presence of the bulky anion BPh_4^- and the large Fe···Fe distance. On the other hand, the spectrum of **1** at 298 K shows quadrupole splitting of $Q.S.$ = 0.886 mms^{-1} with $I.S.$ = 0.280 mms^{-1}. In the temperature range 80–298 K, the $Q.S.$ values decrease on increasing the temperature and no broadening of the full widths at half maximum is observed. The spin state expected from the Mössbauer parameters and magnetic moments (3.70 μ_B) may be in a rapid spin-equilibrium between high- and low-spin states at 298 K. The spectra for rapid intercrossing between high- and low-spin states have been theoretically calculated by Maeda et al.[14] It is expected that the relaxation spectra of an antisymmetric doublet could not be reliably analyzed, and so the interconversion rate for **1**

Table 2. Mössbauer Parameters for the Complexes at 80 and 293 K

Complexes	**1**				**2**			
	I.S. mms^{-1}	*Q.S.* mms^{-1}	Γ_+ mms^{-1}	Γ_- mms^{-1}	*I.S.* mms^{-1}	*Q.S.* mms^{-1}	Γ_+ mms^{-1}	Γ_- mms^{-1}
80 K	0.251	1.525	1.218	0.836	0.235	1.526	1.186	0.793
298 K	0.280	0.886	0.779	0.647	0.194	0.936	0.681	0.654

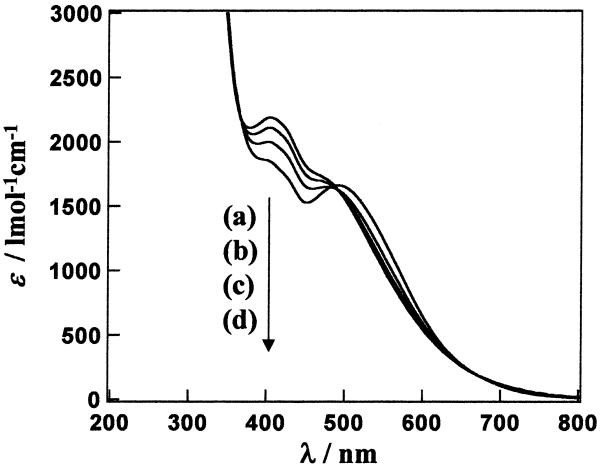

Fig. 4. Temperature dependence of the electronic spectra of **1** in acetonitrile solution; (a): 60 °C, (b): 40 °C, (c): 20 °C, (d): 0 °C.

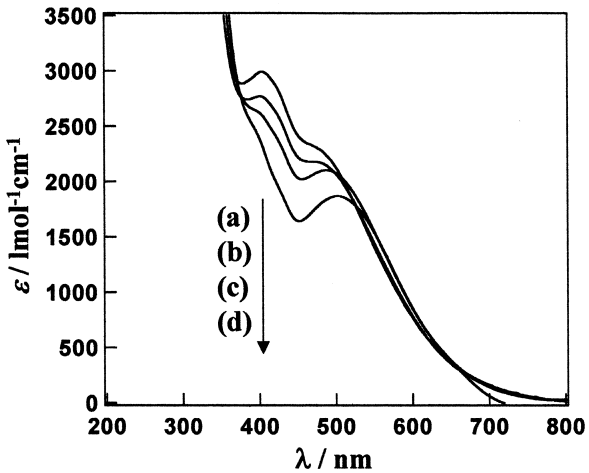

Fig. 5. Temperature dependence of the electronic spectra of **2** in acetonitrile solution; (a): 60 °C, (b): 40 °C, (c): 20 °C, (d): 0 °C.

could not be calculated from the spectra. However, the spectra suggest that the interconversion rate between the high- and low-spin states for **1** (the rate of electronic relaxation of spin transition) is faster than the inverse of the lifetime of the excited states of ^{57}Fe (1×10^7 s^{-1}) at 298 K. Thus the electronic state is in a spin-equilibrium state between the high- and low-spin states. The Mössbauer spectra of **2** are similar to those of **1**; the spectrum shows a large doublet ($Q.S. = 1.526$ mms^{-1}) at 80 K and a small doublet ($Q.S. = 0.936$ mms^{-1}) at 298 K. The spin state expected from the Mössbauer spectrum and the magnetic moments (2.95 μ_B) shows that the compound **2** is in the rapid spin-equilibrium between the high- and low-spin states at 298 K.

Electronic Spectra. The temperature dependence of the electronic spectra was measured in acetonitrile. The binuclear complexes **1** and **2** showed thermochromic behavior. Figure 4 shows the temperature dependence of the spectra for **1**. At 60 °C, the spectrum of **1** exhibits absorptions at 405 and 470 nm, with extinction coefficients (ε) of 2190 and 1740 $lmol^{-1}$ cm^{-1} attributable to ligand-to-metal charge transfer (LMCT) bands. Hauser et al. reported that the bands with the extinction coefficients on the order of 10^3 $lmol^{-1}$ cm^{-1} for iron(III) compounds correspond to the LMCT transitions.[15] On lowering the temperature, the absorption at 405 nm decreases in intensity and that at 470 nm shifts to a longer wavelength. The spectral change is similar to those of the complexes with salten reported previously.[2a,b] The temperature dependence of the electronic spectrum is due to the spin-equilibrium between high- and low-spin states, as is known for the well-characterized spin-crossover ccompounds.[2] The spectral changes are associated with two isosbestic points at 365 and 490 nm. Figure 5 shows the temperature dependence of the spectra for **2**. At 60 °C, the spectrum exhibits bands at 400 and 470 nm; the absorption at 400 nm decreases in intensity with decreasing temperature and that at 470 nm shifts to a longer wavelength, accompanied by the decrease in intensity with lowering the temperature. The temperature dependence of the electronic spectra is also due to the spin-equilibrium between high- and low-spin states. The spectrum changes with a set of isosbestic points at 370 and 520 nm.

Structures of the Complexes. The crystal structures of **1** and **2** were determined by X-ray diffraction at both 298 and 100 K. The space groups ($P2_1/c$ and $P2_1/a$) for **1** and **2** are retained in both of the high- and low-spin states. Figures 6 and 7 show ORTEP views of the molecules together with the numbering of the atoms included in the symmetric unit at 100 K. Each iron atom is surrounded by a nitrogen atom of pyridine, and two oxygen atoms and three nitrogen atoms of a pentadentate salten ligand. The bond lengths and angles corresponding to the intermediate state (298 K) and LS (100 K) forms are compared in Table 3. All of the cell parameters, *a*, *b* and *c*, for **1** and **2** decrease with increasing in temperature, and the volumes of the unit cell decrease 4.15% and 2.66% between 298 and 100 K for **1** and **2**, respectively.

Crystal Structure in the Spin-Equilibrium State. The structures of $[Fe_2(salten)_2(L)](BPh_4)_2$ at 298 K have already been reported.[10] One can briefly notice that the oxgen atoms coordinate to iron atoms in *trans* positions. The values of the bond distances Fe–O (1.89 Å) and Fe–N (2.03 Å) for **1** are intermediate between the typical values of the bond distances for high-spin and low-spin compounds,[15] and the values of the bond distances exhibit also a rapid spin-equilibrium state, as

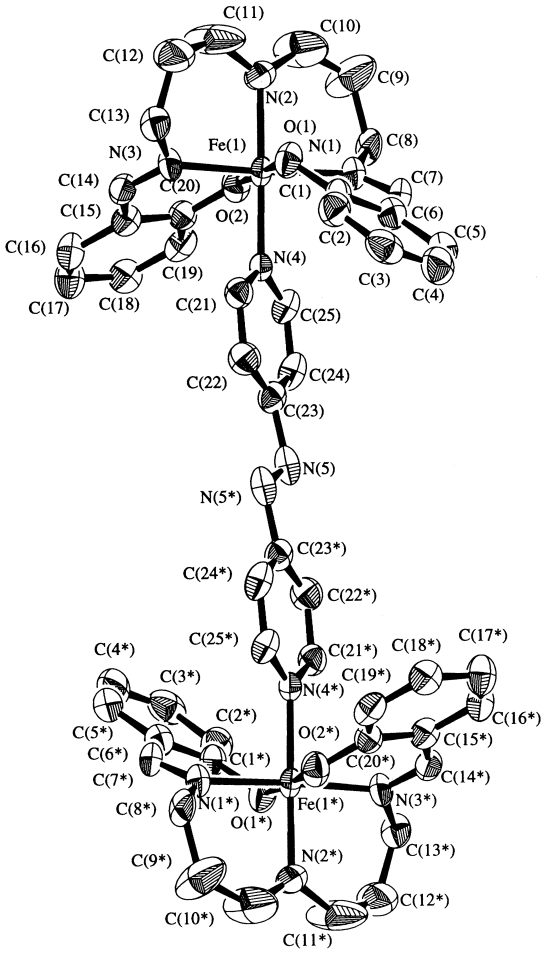

Fig. 6. ORTEP view of $\mathbf{1}^{2+}$ at 100 K showing 50% probability displacement ellipsoids. All hydrogen atoms are omitted for clarity.

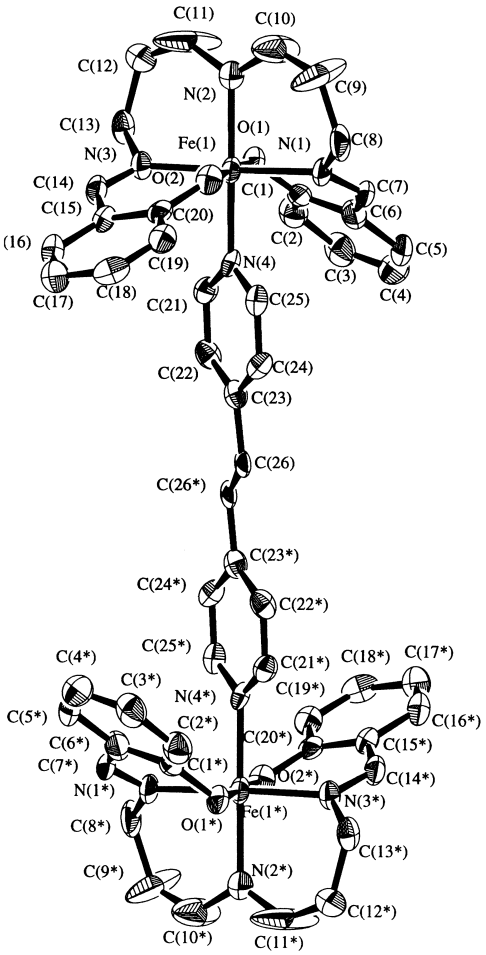

Fig. 7. ORTEP view of $\mathbf{2}^{2+}$ at 100 K showing 50% probability displacement ellipsoids. Some hydrogen atoms are omitted for clarity.

shown from the Mössbauer spectrum for **1** at 298 K. The bond distances Fe–O (1.89 Å) and Fe–N (2.02 Å) for **2** are also intermediate between high- and low-spin states, and the compound **2** is in the spin-equilibrium state at 298 K. The Fe–O distances are shorter than the Fe–N distances, this induces a pronounced distortion of the FeN_4O_2 octahedron. This is also illustrated by O(1)–Fe(1)–O(2) = 176.9(4)° and 177.7(3)°, N(1)–Fe(1)–N(3) = 172.8(6)° and 175.8(3)°, and N(2)–Fe(1)–N(4) = 178.0(5)° and 179.3° for **1** and **2**, respectively (Table 3).

Crystal Structure in the Low-Spin State. At 100 K the arrangements of $[Fe_2(salten)_2(L)](BPh_4)_2$ (**1** and **2**) units are quite similar to that obtained at 298 K. The ORTEP views of the complexes **1** and **2** are shown in Figs. 6 and 7, respectively. The binuclear iron(III) complex is bridged by azobis(4-pyridine). The moiety of diazo (N=N) of the cation of **1** sits on a center of symmetry, two nitrogen atoms of the diazo moiety (N(5) and N(5*)) are a *trans* geometry. The iron atom of the binuclear complex assumes a pseudo-octahedral coordination with a *trans* geometry for the two salicylideneaminato moieties (N(1) and N(3)), in which the basal plane comprises the N_2O_2 donors of these two moieties and the two axial positions are occupied by the secondary amine nitrogen atom of the 3,3′-diaminodipropylamine moiety and the nitrogen atom of azobis(4-pyridine). The basal plane defined by Fe, O(1), O(2), N(1) and N(3) assumes a slight tetrahedral distortion; two oxygen atoms (O(1) and (O(2)) are *trans* to each other, imino nitrogen atoms (N(1) and N(3)) are *trans*, and amine and pyridine nitrogen atoms (N(2) and N(4)) are *trans*. The deviations of the constituent atoms from the least-squares plane FeO_2N_2 are from −0.0207 to 0.0506 Å, and the dihedral angle between the planes Fe–O(1)–N(1) and Fe–O(2)–N(3) is 3.104°. The dihedral angle between two phenyl rings is 118.759° in two salicylideneaminato moieties. The moieties construct a shallow "cave" (or "bow" shape), in which the pyridine unit is positioned, where the depth of the cave can be estimated (by the atom deviations from the FeO_2N_2 basal plane) to be 2.8 Å for C(4) and 1.8 Å for C(17). The values of the bond distances Fe–O (1.87 Å) and Fe–N (1.97 Å) are typical values of the bond distances for low-spin compounds. The spin transition affects principally the FeN_4O_2 core geometry. The Fe–O bonds in low-spin form are shorter by 0.013 Å and the Fe–N bonds by about 0.056 Å as compared to those in the spin-equilibrium state for **1**. The structure of **2** is similar to that of **1**, and the binuclear iron(III) complex is bridged by 4,4′-vinylenebis(pyridine). The vinylene group has *trans* geometry

Table 3. Representative Bond Distances (Å) and Angles (°) for the Complexes

Complexes	**1**		2	
	T = 298 K	T = 100 K	T = 298 K	T = 100 K
		Bond distances (Å)		
Fe(1)–O(1)	1.893(8)	1.866(4)	1.886(5)	1.867(5)
Fe(1)–O(2)	1.890(9)	1.881(4)	1.892(5)	1.889(5)
Fe(1)–N(1)	2.05(1)	1.963(5)	1.989(6)	1.975(6)
Fe(1)–N(2)	2.02(1)	2.000(5)	2.065(6)	2.011(6)
Fe(1)–N(3)	2.01(1)	1.944(5)	2.000(6)	1.952(6)
Fe(1)–N(4)	2.037(10)	1.988(4)	2.045(6)	2.006(6)
		Bond angles (°)		
O(1)–Fe(1)–O(2)	176.9(4)	177.8(2)	177.7(3)	179.4(2)
O(1)–Fe(1)–N(1)	89.1(5)	88.9(2)	90.6(2)	89.8(3)
O(1)–Fe(1)–N(2)	91.9(4)	90.9(2)	92.6(3)	89.3(2)
O(1)–Fe(1)–N(3)	89.8(4)	90.1(2)	89.9(2)	90.0(2)
O(1)–Fe(1)–N(4)	88.4(4)	89.4(2)	87.9(2)	90.7(2)
O(2)–Fe(1)–N(1)	89.1(5)	89.3(2)	90.3(2)	89.8(3)
O(2)–Fe(1)–N(2)	90.7(5)	90.4(2)	89.6(3)	91.2(2)
O(2)–Fe(1)–N(3)	92.2(4)	91.7(2)	89.3(2)	90.4(2)
O(2)–Fe(1)–N(4)	89.1(4)	89.3(2)	89.9(2)	88.8(2)
N(1)–Fe(1)–N(2)	87.3(6)	89.4(2)	87.3(3)	89.5(3)
N(1)–Fe(1)–N(3)	172.8(6)	177.0(2)	175.8(3)	178.1(3)
N(1)–Fe(1)–N(4)	94.6(6)	91.3(2)	92.3(3)	90.8(3)
N(2)–Fe(1)–N(3)	85.6(6)	87.7(2)	88.6(3)	88.6(3)
N(2)–Fe(1)–N(4)	178.0(5)	179.2(2)	179.3(2)	179.7(3)
N(3)–Fe(1)–N(4)	92.5(5)	91.6(2)	91.8(3)	91.1(3)

(C(26) and C(26*)). The FeO_2N_2 basal plane shows a slight tetrahedral distortion, with two oxygen atoms (O(1) and (O(2)) being *trans* to each other, imino nitrogen atoms (N(1) and N(3)) being *trans*, and amine and pyridine nitrogen atoms (N(2) and N(4)) being *trans*. The deviations of the constituent atoms from the least-squares plane FeO_2N_2 are from −0.0337 to 0.0091 Å, and the dihedral angle between the planes Fe–O(1)–N(1) and Fe–O(2)–N(3) is 1.955°. The dihedral angle between two phenyl rings is 115.847° in two salicylideneaminato moieties. The moieties construct a cave as with **1** in which the pyridine unit is positioned; the depth of the cave can be estimated (by the atom deviations from the FeO_2N_2 basal plane) to be 2.8 Å for C(4) and 2.0 Å for C(17). The values of the bond distances Fe–O (1.88 Å) and Fe–N (1.99 Å) are intermediate between the typical values of the bond distances for low-spin compounds, too. Similarly, the Fe–O bonds in low-spin form are shorter by 0.011 Å and the Fe–N bonds by about 0.039 Å as compared to those in the spin-equilibrium state for **2**. It can be considered that a slight conformational change of the chelate rings reflects the tetrahedral distortion of the FeO_2N_2 basal plane and the iron-ligand bond lengths, and as a result it induces the spin transition.

Pressure-Stabilized Low-Spin State. The temperature dependences of the effective magnetic moments for the complexes **1** and **2** were measured on single crystals in the temperature range from 1.8 to 350 K and results are shown in Figs. 8 and 9, respectively. At ambient pressure, the complexes **1** and **2** are in the low-spin state below 200 K and in the rapid spin-equilibrium state at room temperature, as previously described (Fig. 1). At 8 kbar, the magnetic moments of **1** and **2** are ca. 2.0 μ_B, and the low-spin state is stabilized even at 350 K. On warming, the moments of **1** and **2** slightly increase to

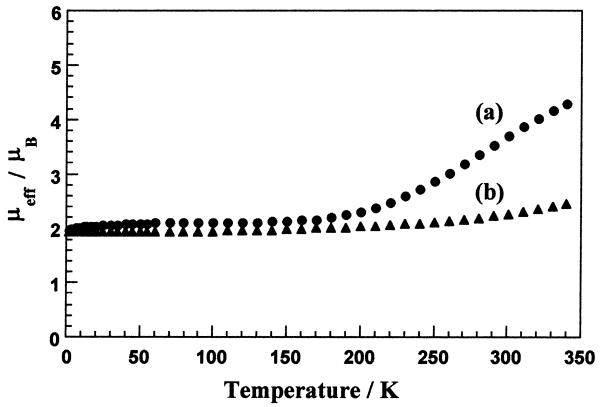

Fig. 8. Temperature dependence of the effective magnetic moments of **1** under 1 bar (a) and 8 kbar (b).

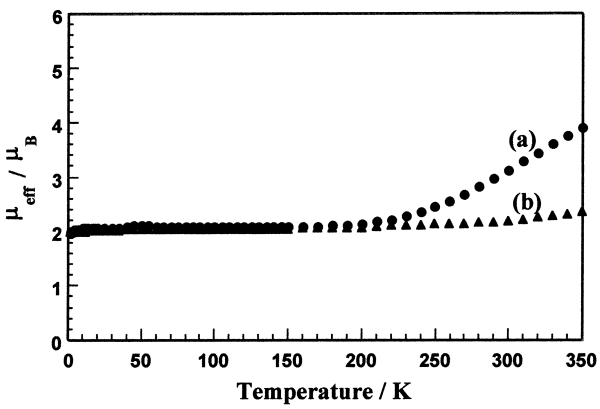

Fig. 9. Temperature dependence of the effective magnetic moments of **2** under 1 bar (a) and 8 kbar (b).

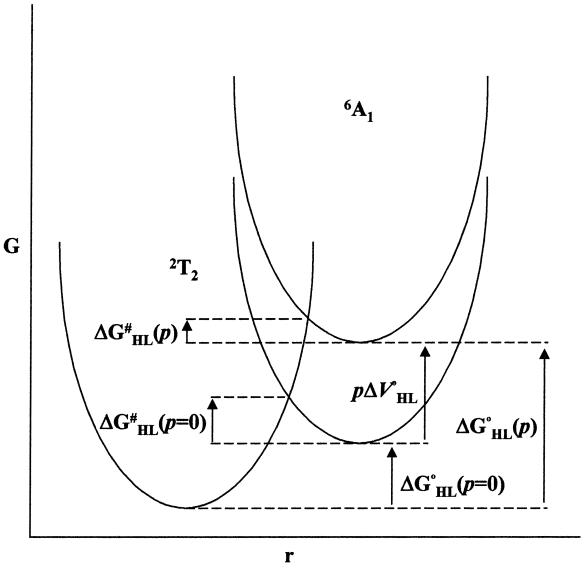

Fig. 10. Schematic representation of the influence of pressure on the low-spin state ($^2T_2$) and high-spin state ($^6A_1$). Pressure increases the zero point energy difference, $\Delta G^{\circ}_{HL}(p)$ by the work term $p\Delta V^{\circ}_{HL}$ and decreases the activation energy $\Delta G^{\#}_{HL}(p)$, thus favouring the low-spin state and increasing the rate constant k_{HL}.

ca. 2.2 μ_B at 350 K. The application of pressure to the high-spin systems first decreases the volume of the crystal unit cell, which leads to a shortening of intermolecular spacing and then to an increase of the lattice strain. When the pressure becomes high enough to force a structural rearrangement to occur, then the low-spin species where the lattice strain is weaker due to the smaller volume of molecules, is thermodynamically stabilized and a spin-equilibrium → low-spin transition takes place. Figure 10 shows the influence of pressure on the low-spin state ($^2T_2$) and high-spin state ($^6A_1$). The spin-crossover iron(Ⅲ) complexes are suited for pressure studies because the difference in volume: $\Delta V^{\circ}_{HL} = V_{HS} - V_{LS}$, between HS and LS complexes is due to the difference in metal-ligand bond lengths: $\Delta r^{\circ}_{HL} = r_{HS} - r_{LS} \approx 0.10$ Å. Therefore, the external pressure gives the work term, $p\Delta V^{\circ}_{HL}$, to the Gibbs' free energy and thus influences both the thermal spin transition as well as inter-system-crossing dynamics substantially. For **1** and **2**, the thermal spin transition occurs gradually with a transition temperature $T_{1/2}$ of ca. 300 K at normal pressure, and there are no indications of a crystallographic phase transition. When pressure is applied $T_{1/2}$ increases to higher temperature. This is due to a small decrease in the bond length of the metal-ligand in the low-spin state with pressure and the resulting increasing in ligand-field strength of 10 Dq.

Conclusions

Binuclear iron(Ⅲ) complexes with bridging photoisomerization ligands az or cc are prepared; they exhibit spin-crossover behavior depending on temperature. The Mössbauer spectra for **1** and **2** show a doublet at 293 K, suggesting the rapid spin-equilibrium between high- and low-spin states. The average bond lengths of Fe–O and Fe–N for **1** and **2** are intermediate between the typical values of the bond lengths for high- and low-spin complexes. Both of the complexes exhibit the low-spin state under 8 kbar at room temperature.

We thank Prof. J.-P. Tuchagues (University of Paul Sabatier I, Toulouse Cedex, France) for kind suggestions about this work.

Supplementary Material Available:

Tables of full crystal data, calculated hydrogen atom positions, anisotropic thermal parameters, and completed bond lengths and angles for $[Fe_2(salten)_2(az)](BPh_4)_2$ (**1**) and $[Fe_2(salten)_2(cc)](BPh_4)_2$ (**2**). Ordering information is given on any current masthead page.

References

1 a) H. A. Goodwin, *Coord. Chem. Rev.*, **18**, 293 (1976). b) P. Gütlich, *Struct. Bonding (Berlin)*, **44**, 83 (1981). c) P. Gütlich and A. Hauser, *Coord. Chem. Rev.*, **97**, 1 (1990). d) E. König, *Prog. Inorg. Chem.*, **35**, 527 (1987). e) E. König, *Struct. Bonding (Berlin)*, **76**, 51 (1991). f) D. Boinnard, A. Bousseksou, A. Dworkin, J.-M. Savariault, F. Varret, and J.-P. Tuchagues, *Inorg. Chem.*, **33**, 271 (1994). g) J. Kröber, E. Codjovi, O. Kahn, F. Groliére, and C. Jay, *J. Am. Chem. Soc.*, **115**, 9810 (1993).

2 a) N. Matsumoto, S. Ohta, C. Yoshimura, A. Ohyoshi, S. Kohata, H. Okawa, and Y. Maeda, *J. Chem. Soc., Dalton Trans.*, **1985**, 2575. b) S. Ohta, C. Yoshimura, N. Matsumoto, H. Okawa, and A Ohyoshi, *Bull. Chem. Soc. Jpn.*, **59**, 155 (1986). c) Y. Maeda, H. Ohshio, Y. Takashima, M. Mikuriya, and M. Hidaka, *Inorg. Chem.*, **25**, 2958 (1986). d) H. Ohshio, Y. Maeda, and Y. Takashima, *Inorg. Chem.*, **22**, 2684 (1983).

3 a) S. Usha, R. Srinivasan, and C. N. R. Rao, *Chem. Phys.*, **100**, 447 (1985). b) M. Konno and M. Mikami-Kido, *Bull. Chem. Soc. Jpn.*, **64**, 339 (1991). c) W. S. Hammack, A. J. Conti, D. N. Hendrickson, and H. G. Drickamer, *J. Am. Chem. Soc.*, **111**, 1738 (1989). d) C. Roux, J. Zarembowitch, J. P. Itié, M. Verdaguer, E. Dartyge, A. Fontaine, and H. Tolentino, *Inorg. Chem.*, **30**, 3174 (1991). e) E. König, G. Ritter, H. Grünsteudel, J. Dengler, and J. Nelson, *Inorg. Chem.*, **33**, 837 (1994). f) C. Roux, J. Zarembowitch, J. P. Itié, A. Polian, and M. Verdaguer, *Inorg. Chem.*, **35**, 574 (1996).

4 a) S. Decurtins, P. Gütlich, C. P. Köhler, H. Spiering, and A. Hauser, *Chem. Phys. Lett.*, **105**, 1 (1984). b) S. Decurtins, P. Gütlich, K. M. Hasselbach, A. Hauser, and H. Spiering, *Inorg. Chem.*, **24**, 2174 (1985). c) P. Gütlich, A. Hauser, and H. Spiering, *Angew. Chem., Int. Ed. Engl.*, **33**, 2024 (1994).

5 S. Schenker, A. Hauser, and R. Dyson, *Inorg. Chem.*, **35**, 4676 (1996).

6 a) C. Roux, J. Zarembowitch, B. Gallois, and M. Bolte, *New J. Chem.*, **16**, 671 (1992). b) C. Roux, J. Zarembowitch, B. Gallois, T. Granier, and R. Claude, *Inorg. Chem.*, **33**, 2273 (1994). c) M.-L. Boillot, C. Roux, J.-P. Audiére, A. Dausse, and J. Zarembowitch, *Inorg. Chem.*, **35**, 3975 (1996).

7 a) J. A. Real, E. Andrés, M. C. Muñoz, M. Julve, T. Granier, A. Bousseksou, and F. Varret, *Science*, **268**, 265 (1995). b) K. Hamachi, K. Matsuda, and H. Iwamura, *Bull. Chem. Soc. Jpn.*, **71**, 2937 (1998).

8 a) J. Jeftić, H. Romstedt, and A. Hauser, *J. Phys. Chem. Solids*, **57**, 1743 (1996). b) J. Jeftić and A. Hauser, *J. Phys. Chem. B*, **101**, 10262 (1997).

9 Y. Garcia, V. Ksenofontov, G. Levchenko, G. Schmitt, and P. Gütlich, *J. Phys. Chem. B*, **104**, 5045 (2000).

10 a) S. Hayami, K. Inoue, S. Osaki, and Y. Maeda, *Chem. Lett.*, **1998**, 987. b) S. Hayami, K. Inoue, and Y. Maeda, *Mol. Cryst. Liq. Cryst.*, **335**, 573 (1999).

11 D. A. Baldwin, A. B. P. Lever, and R. V. Parish, *Inorg. Chem.*, **8**, 107 (1969).

12 Microanalyses for carbon, hydrogen and nitrogen were carried out by the Elemental Analysis Center, Kyushu University.

13 Y. Hosokoshi, M. Tamura, and M. Kinoshita, *Mol. Cryst. Liq. Cryst.*, **306**, 423 (1997).

14 Y. Maeda, H. Ohshio, and Y. Takashima, *Chem. Lett.*, **1982**, 943.

15 S. Schenker, A. Hauser, and R. M. Dyson, *Inorg. Chem.*, **35**, 4676 (1996).

16 S. Hayami, T. Matoba, S. Nomiyama, T. Kojima, S. Osaki, and Y. Maeda, *Bull. Chem. Soc. Jpn.*, **70**, 3001 (1997).